Int. J. Electrochem. Sci., 8 **(2013)** 11228 - 11247

International Journal of ELECTROCHEMICAL SCIENCE
www.electrochemsci.org

Experimental, Quantum Chemical and Molecular Dynamics Studies of Imidazoline Molecules Against the Corrosion of Steel and Quantitative Structure- Activity Relationship Analysis Using the Support Vector Machine (SVM) Method

Haixiang Hu[1], *Lei Du*[2], *Xiaochun Li*[1*], *Hongxia Zhao*[3], *Xiuhui Zhang*[3,*],*Shumin Shi*[4], *Hanlai Li*[5], *Xiaoyong Tang*[2], *Jing Yang*[2]

[1]State Key Laboratory of Geomechanics and Geotechnical Engineering, Chinese Academy of Sciences, Institute of Rock and Soil Mechanics, 12th, Xiaohongshan, Wuchang, Wuhan, Hubei 430071, P.R. China
[2] China Petroleum Engineering Southwest Company, Chengdu 610041, P. R. China
[3] Key Laboratory of Cluster Science, Ministry of Education of China, School of Chemistry, Beijing Institute of Technology, Beijing 100081, P. R. China
[4] School of Computer Science & Technology, Beijing Institute of Technology, Beijing 100081, P. R. China
[5]Department of Chemistry, Capital Normal University, Beijing, 100048, P. R. China P. R. China
[*]E-mail: xcli@whrsm.ac.cn; zhangxiuhui@bit.edu.cn

Received: 16 May 2013 / *Accepted:* 3 July 2013 / *Published:* 20 August 2013

The inhibition performance of nine imidazoline molecules against the corrosion of steel in 15 wt.% HCl and 3 wt.% HF solution was studied by weight-loss method, quantum chemical calculation, molecular dynamics simulation and the quantitative structure−activity relationship (QSAR) analysis. The quantum chemical calculation involved in local reactivity suggested that the nitrogen atoms in the imidazole ring and carbon atoms in hydrophilic group were the possible active sites to be adsorbed on iron surface. The acid solution was taken into consideration in molecular dynamics simulation and the results indicated that the order of the binding energies agrees well with that of the inhibition efficiencies. The QSAR model was built by the support vector machine (SVM) approach to correlate between the inhibition efficiencies of the imidazoline molecules and their quantum chemical parameters as well as the binding energies. The QSAR model shows good performance since the value of correlation coefficient R^2 was reasonably high. What's more, eight new imidazoline molecules were theoretically designed and their inhibition efficiencies were predicted by the established QSAR model.

Keywords: imidazoline molecules, weight-loss method, DFT, molecular dynamics simulation, QSAR

1. INTRODUCTION

Metals and alloys, especially the mild steel, are used widely in industrial fields. At the same time, the corrosion of metals usually results in huge financial losses and many potential safety issues. Adding the corrosion inhibitors into the oil can be regarded as one of the most convenient and economic methods among the various anticorrosion measures, because corrosion inhibitors can slow down corrosion rate or protect metal from corrupting, though used in a very small amount [1-3]. Most of the efficient corrosion inhibitors are compounds containing heteroatoms with lone pair of electrons (e.g., N, O, S and P), or π-systems, or conjugated bonds, or aromatic systems [4]. Imidazoline and its derivatives are such kind of compounds that can be against the corrosion of CO_2 and H_2S effectively [5-6]. Moreover, they are environmental friendly due to their biodegradability [7].

Many studies about imidazoline and its derivatives have been carried out including experimental and theoretical investigations. For the experimental researches, many measures, such as weight-loss method, potentiodynamic polarization, electrochemical impedance spectroscopy (EIS), scanning electron microscope (SEM) and atomic force microscopy (AFM), were usually used to study the inhibition efficiency and inhibition process of imidazoline molecule under different conditions [8-13]. For the theoretical studies, quantum computational method and molecular dynamics simulation were usually employed to obtain the molecular properties and the corrosion inhibition mechanism [14-18]. For example, J. Cruz [15] studied a series of imidazoline molecules using the quantum computational method and found that the global reactivity indices together with the local reactivity indices were helpful to explain the performance of imidazolines as a corrosion inhibitor. S. Xia [18] investigated two imidazoline molecules using quantum chemistry method and molecular dynamics simulation and found that imidazoline molecules can be adsorbed on the Fe surface in vacuum or in water through the imidazoline ring and heteroatoms. In addition, linear or simple non-linear quantitative structure-activity relationship (QSAR) models were also built to research the relationship between inhibition efficiency and some related quantum chemical parameters [19].

Though the extensive studies of imidazoline inhibitors have been carried out by experimental and theoretical approaches, many problems in the corrosion inhibition process are still unclear. For molecular dynamics studies, few researchers have taken the electrolyte anions in corrosion solution into consideration, which have great influence on the performance of corrosion inhibitors, such as chloride ion [20]. For the QSAR studies, considering the performance of the corrosion inhibitors was affected by many factors and it can't be explained by linear or simple non-linear QSAR model [21-22]. Thus, advanced and suitable approaches, such as neural network approach (NNA) or the support vector machine (SVM) should be selected. The reliable correlation between the structural characters and activities or properties will help us to accurately predict the performance the new corrosion inhibitors.

In this study, the inhibition performances of a series of imidazoline compounds have been studied via weight-loss method together with the quantum chemistry and molecular dynamics simulation. A QSAR model was built by the support vector machine (SVM) approach. What's more, eight new imidazoline molecules were theoretically designed and their inhibition efficiencies were predicted by the established QSAR model.

2. EXPERIMENTAL

2.1. Materials

Nine imidazoline molecules were studied in present study and their molecular structures and the sequencing of some atoms were shown in Table 1. All the structures of the nine imidazoline molecules include a five membered ring containing two nitrogen atoms, a hydrophilic group and a hydrophobic group. There are two kinds of hydrophilic groups, namely $-CH_2CH_2NH_2$ (for molecules 1, 4, 6, 8,) and $-(CH_2CH_2NH)_2CH_2CH_2NH_2$ (for the molecules 2, 3, 5, 7, 9). While for the hydrophobic groups, hydrocarbon straight-chains are for the molecules 1-7, and benzene ring for molecules 8 and 9.

Table 1. Structures and sequencing of atoms of nine imidazoline molecules

Inhibitor	Structure	Inhibitor	Structure
1	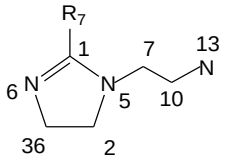 $R_7 = -C_7H_{15}$	2	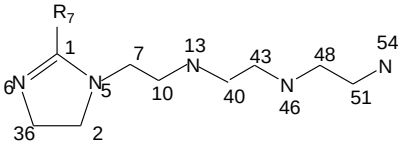 $R_7 = -C_7H_{15}$
3	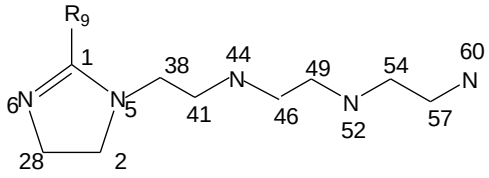 $R_9 = -C_9H_{19}$	4	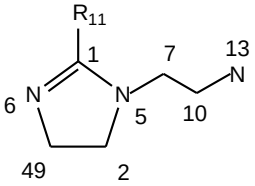 $R_{11} = -C_{11}H_{23}$
5	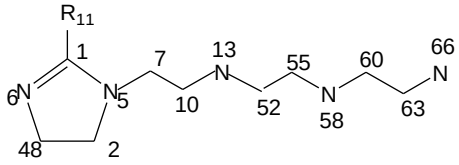 $R_{11} = -C_{11}H_{23}$	6	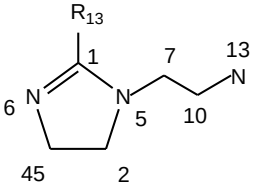 $R_{13} = -C_{13}H_{27}$
7	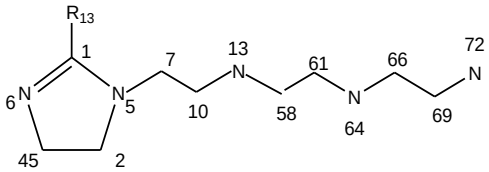 $R_{13} = -C_{13}H_{27}$	8	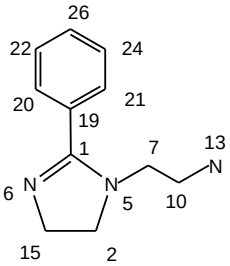
9	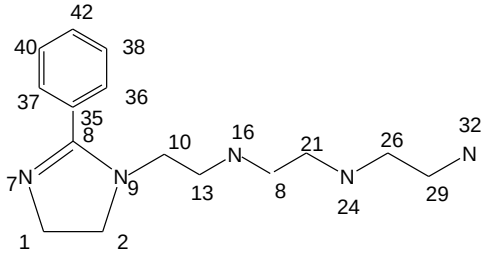		

2.2. Weight-loss method

Weight loss testing was performed on X52 steel with dimension of 50×10×2mm. Before testing, all steel specimens were abraded with sandpapers, cleaned with double distilled water and absolute ethyl alcohol, dried in a drier and weighted as m_1. Then, steel specimens were immersed in 15 wt.% HCl and 3 wt.% HF solution with corrosion inhibitors at concentration of 400 ppm at 60°C for 4 h. At the same time, a blank test was also carried out without corrosion inhibitors under the same conditions. After testing, each specimen was taken out and then cleaned with double distilled water and absolute ethyl alcohol, dried in a drier. Specimens immersed in solution with and without corrosion inhibitors were weighted as m_2 and m_3, respectively. The inhibition efficiency (IE) was calculated using the following equations [18]:

$V= (m_1-m_2)/(S\times t)$

$V_0= (m_1-m_3)/(S\times t)$

$IE = (V_0 -V)/V_0\times 100\%$

Where S is the surface area of specimen; t is response time; V is corrosion rate with corrosion inhibitors; V_0 is corrosion rate without corrosion inhibitors.

2.3 Quantum chemistry calculation

The quantum chemical calculation were performed with Gaussian09 program package [23] at the B3LYP/6-311+G (d,p) level of theory. The B3LYP method shows a good estimate of molecular properties which are related to the molecular reactivity [24]. The considered quantum chemical parameters include energy of the highest occupied molecular orbital (E_{HOMO}), energy of the lowest unoccupied molecular orbital (E_{LUMO}), dipole moment (μ), the change in the number of electrons transferred (ΔN), the adiabatic ionization potential (AIP), the vertical ionization potential (VIP), the vertical electron affinity (EA_{vert}) and so on. The adiabatic ionization potential (AIP) and the vertical ionization potential (VIP) [25] are estimated in the following manner:

AIP = E(optimized cation)-E(optimized neutral)

VIP= E(cation at optimized neutral geometry) −E(optimized neutral)

The vertical electron affinity(EA_{vert}) [26] are estimated in the following manner:

EA_{vert}=E(optimized neutral)−E(anion at optimized neutral geometry)

The change in the number of electrons transferred [27] ΔN and ΔN_{vert} were estimated through the equations:

$\Delta N=(\chi_{Fe}-\chi_{inh})/2(\eta_{Fe}-\eta_{inh})$

$\Delta N_{vert}=(\chi_{Fe}-\chi_{inh,vert})/2(\eta_{Fe}-\eta_{inh,vert})$

$\chi_{inh}=-(E_{LUMO}+E_{HOMO})/2$ (1)

$\eta_{inh}=(E_{LUMO}-E_{HOMO})/2$ (2)

$\chi_{inh,vert}=(VIP +EA_{vert})/2$ (3)

$\eta_{inh,vert}=(VIP-EA_{vert})/2$ (4)

Where the values of χ_{Fe} and η_{Fe} are taken as 7eVmol^{-1} and 0 eVmol^{-1}, respectively [28]. The values of χ_{inh} and η_{inh} are calculated from equation (1) and equation (2), respectively. And the values of $\chi_{inh,vert}$ and $\eta_{inh,vert}$ are calculated from equation(3) and equation(4), respectively.

Natural bond orbital (NBO) analysis [29] was performed to evaluate the electron-density distributions. The electron density plays an important role in estimating the chemical reactivity. The local reactivity has been analyzed by means of Fukui indices and contribution to HOMO or LUMO of atoms. The condensed Fukui [30] functions are calculated from the natural charge analysis of atoms and it was expressed as follows：

$f^{+}_{k}= q_k(N+1)-q_k(N)$ (for nucleophilic attack)

$f^{-}_{k}= q_k(N)-q_k(N-1)$ (for electrophilic attack)

where q_{N+1}, q_N, and q_{N-1} are the charges of the atoms on the systems with N +1, N, and N − 1 electrons, respectively. To certain molecules, contribution of each atom to HOMO or LUMO is proportional to the square of the HOMO or LUMO coefficients [31]. Corresponding contribution to HOMO or LUMO can be expressed as:

$$\chi^{r}_{HOMO} = \frac{\sum_{i}(C^{r}_{i,HOMO})^2}{\sum_{r}\sum_{i}(C^{r}_{i,HOMO})^2} \quad \chi^{r}_{LUMO} = \frac{\sum_{i}(C^{r}_{i,LUMO})^2}{\sum_{r}\sum_{i}(C^{r}_{i,LUMO})^2}$$

2.4 Molecular dynamics simulation

The molecular dynamics(MD) simulation of the interaction between imidazoline molecules and iron surface in acid solution were performed using Materials Studio 5.5 program developed by Accelrys Inc [32]. The Amorphous Cell module and Forcite module were used. The Amorphous Cell [33] module allows constructing complex systems and the Forcite module [32] allows geometry optimization and energy calculation of periodic systems. The MD simulation was carried out in a simulation box (2.98nm×2.98nm×9.76nm) with periodic boundary conditions. The box includes a Fe slab, an acid solution layer and a vacuum layer. In acidic solution, -NH_2 have a great tendency to be protonated. Thus, the protonated imidazoline molecules are considered in the simulation. Moreover, in order to build a model in accord with the real experimental solution, both waters and hydrogen chloride were considered, and the adsorption system includes 746 H_2O, 54 H_3O^+, 55 Cl^- and 1 protonated inhibitor molecule. Then, the acid solution layer was simulated with density of 1.011 g/cm^{-3}, which was calculated by dynamics simulation under NPT ensemble for 200 ps to obtain the equilibrium status of systems at a temperature of 298K and at a pressure of 0.1 MPa controlled by Andersen thermostat and Berendsen Barostat, respectively [33]. As for the iron surface, Fe (1 1 0) is a density packed surface and has the most stabilization, so Fe (1 1 0) was chosen as the adsorption surface [34]. The iron surface includes 13 layers, and 10 layers near the bottom were frozen. The MD simulation was performed at 298 K controlled by the Andersen thermostat, NVT ensemble, with a time step of 1.0 fs and simulation time of 2000ps using the compass force field. Interactions of non-bond for each system, van der Waals and electrostatic, were computed by atom-based summation method and Ewald summation method, respectively, with a cutoff radius of 1.55 nm.

2.5 Quantitative structure and activity relationship (QSAR)

In the present study, the support vector machine (SVM) [35] approach has been used to build a quantitative structure and activity relationship (QSAR) to investigate the relationship of inhibition efficiencis of the imidazoline molecules and their quantum chemical parameters as well as combining energies. The support vector machine (SVM) is a relatively novel machine learning technique based on a statistical learning theory (SLT) principle [35]. It has been extended to solve regression problems, and has good performance in QSAR studies due to its extraordinary capability [36] . Compared with other learning machines, such as artificial neural networks, SVM has smaller standard error [37]. For SVM, we used freely available LIBSVM software [37]. All calculations were performed using the MATLAB package.

3. RESULTS AND DISCUSSION

3.1 Experimental results

The results of inhibition efficiencies in 15 wt. % HCl and 3 wt. % HF solution with corrosion inhibitor concentration of 400 ppm at 60°C for 4 h tested by weight-loss method are shown in Table2. For the imidazoline molecules with hydrocarbon straight-chain, namely molecules 1-7, the inhibition efficiencies are from 26.34% to 95.39%, which are not always increase with the increasing of the lengths of hydrocarbon straight-chain. While for those contain benzene rings (molecules 8-9), the inhibition efficiencies are less than 60%. In addition, for the imidazoline molecules with the same hydrophobic groups, it is interesting to found that the inhibition efficiencies of molecules with –$(CH_2CH_2NH)_2CH_2CH_2NH_2$ are higher than those with -$CH_2CH_2NH_2$.

Table 2. Experimental inhibition efficiencies of nine imidazoline molecules

Inhibitor	Inhibition efficiency (%)	Inhibitor	Inhibition efficiency (%)
1	26.34	6	60.64
2	87.71	7	57.67
3	91.59	8	20.62
4	77.86	9	59.01
5	95.39		

3.2 Global reactivity

Chemical reactivity of compounds is related to its structural characteristics, which can be expressed clearly by their quantum chemical parameters. The selected parameters include E_{HOMO}, E_{LUMO}, dipole moment (μ), the adiabatic ionization potential (AIP), the vertical ionization potential (VIP) etc. Table 3 presents all the calculated quantum chemical parameters of the imidazoline molecules.

E_{HOMO} is associated with the electron donating ability of a molecule. The higher value of the E_{HOMO} is, the greater tendency of a molecule has to donate electrons [38]. On the contrary, E_{LUMO} indicates the ability to accept electrons. Lower value of E_{LUMO} has a greater tendency to accept electrons [39]. As shown in Table 3, molecule 2 with the highest E_{HOMO} and molecule 8 with the lowest E_{LUMO} provide an indication that the molecule 2 has the greatest ability to donate electrons and molecule 8 are easy to accept electrons. However, the results of E_{HOMO} and E_{LUMO} do not agree completely with the trends in the inhibition efficiencies of all the compounds.

Table 3. Quantum chemical parameters of nine imidazoline molecules at the B3LYP/6-311+G(d,p) level of theory and experimental inhibition efficiencies

Inhibitor	E_{homo} /eV	E_{lumo} /eV	μ/Debye	α	Q_{total}/C	Q_{ring}/C	Z_{total}/C	Z_{ring}/C
1	-5.904	-0.258	1.952	170.630	-5.579	-1.001	-4.456	0.090
2	-5.767	-0.178	4.270	237.740	-7.703	-0.999	-5.507	-0.344
3	-5.785	-0.221	4.566	265.060	-8.403	-1.000	-5.813	-0.523
4	-5.847	-0.212	2.900	220.040	-7.080	-1.000	-5.314	-0.208
5	-5.818	-0.137	4.249	290.010	-9.154	-0.999	-6.733	-0.101
6	-5.894	-0.257	1.956	245.700	-7.834	-1.001	-6.043	-0.023
7	-5.845	-0.193	2.930	314.300	-9.963	-1.360	-7.209	-0.371
8	-5.982	-1.075	1.939	153.370	-3.708	-0.995	-2.948	-0.561
9	-5.933	-0.989	4.367	222.640	-5.782	-0.990	-4.271	-0.393

Table 3.(continued). Quantum chemical parameters of nine imidazoline molecules at the B3LYP/6-311+G(d,p) level of theory and experimental inhibition efficiencies

V/cm^3mol^{-1}	AIP/eV	VIP/eV	EA_{vert} /eV	ΔNvert	ΔN	E_{ad} /kcal*mol^{-1}	IE/%
133.454	7.235	7.751	-0.735	0.412	0.694	-125.32	26.342
185.528	6.783	7.284	-0.695	0.464	0.721	-175.50	87.711
204.755	6.956	7.362	-0.611	0.455	0.718	-189.92	91.591
171.909	7.229	7.765	-0.711	0.410	0.705	-161.99	77.864
223.982	7.062	7.371	-0.822	0.455	0.708	-207.26	95.390
191.136	7.224	7.723	-0.712	0.414	0.696	-178.43	60.637
243.209	6.868	7.265	-0.725	0.467	0.704	-225.04	57.667
103.154	7.265	7.689	-0.491	0.416	0.707	-106.60	20.622
155.227	7.039	7.350	-0.356	0.455	0.716	-160.28	59.007

The dipole moment (μ) and polarizability (α) indicate the polarity of a molecule and they are good reactivity indicators [40]. The bigger value of the dipole moment and the polarizability, the more possible for the molecule to change its original shape and the greater tendency the molecule will has to be absorbed on metal surface. Molecular volume indicates possible surface coverage by the corrosion inhibitors. The larger molecular volume (V) of a corrosion inhibitor has, the bigger surface coverage will be formed on metal surface, which was favor to corrosion protection [41]. Table 3 shows that molecule 9 has the greatest dipole moment, and molecule 7 has the greatest polarizability and the largest volume, which indicates that these molecules are easy to be absorbed on metal surface, but their experimental efficiencies are not the highest. As to molecule 5, it shows the highest experimental

efficiency and the value of its dipole moment, polarizability and volume are greater than most of molecules.

Total negative charges of all non-hydrogen atoms in imidazoline molecule, Q_{total}(natural charge) and Z_{total}(Mulliken charge), total charges of all non-hydrogen atoms in imidazole ring, Q_{ring}(natural charge) and Z_{ring}(Mulliken charge), are listed in Table 3. The absolute values of Q_{total}, Z_{total}, Q_{ring} and Z_{ring} are related to chemical reactivity[40,42], and, as shown in Table 3, molecule 7 have the highest absolute values of Q_{total}, Z_{total}, Q_{ring} and Z_{ring}. It is suggested that this molecule has the greatest chemical reactivity. However, the inhibition efficiency of molecular 7 is not very high. An analysis of the absolute values of Q_{total}, Z_{total}, Q_{ring} and Z_{ring} of all the molecules and their corresponding inhibition efficiencies indicates that the order of the absolute values of Q_{total}, Z_{total}, Q_{ring} and Z_{ring} do not agree with the trends in the experimental inhibition efficiencies very well.

The change in the number of electrons transferred ΔN or ΔN_{vert} indicates the tendency of a molecule to donate electrons [41]. Though ΔN values are not exactly the number of electrons transferring from the donor to the acceptor molecule, it is more adequate to indicate the ability of electron-donating [43]. As tabulated in the Table 3, molecules 2 have the highest values of ΔN, which indicates the greatest ability to donate electrons. It is in accord with the results of E_{HOMO}. However, the trend of the ΔN or ΔN_{vert} values does not correlate well with the experimental inhibition efficiencies.

From the discussion above, it can be concluded that all these quantum chemical parameters are related to the chemical reactivity of these imidazoline molecules. However, due to the complexity of the corrosion protection, the inhibition performance is affected by many factors, which causes the order of each parameter does not correlate well with the trend of the inhibition efficiencies. Therefore, all the quantum chemical parameters will be taken into consideration to build QSAR model.

3.3 Local reactivity

According to the frontier molecular orbital theory (FMO) [44], the chemical reactivity is closely related to HOMO and LUMO of the reacting species. The figures of HOMO and LUMO of all imidazoline molecules are shown in Figure1. For molecules1-7, HOMOs are located in the imidazole ring and hydrophilic group and LUMOs' location are concentrated on hydrophilic group. As to molecules 8 and 9, HOMOs are located in imidazole ring and hydrophilic group and LUMOs in the imidazole ring and benzene ring. These results indicate that the reactive regions of imidazoline molecules are not correlative with the hydrocarbon straight-chain.

In order to confirm the active sites, these nine imidazoline molecules were researched by the condensed Fukui function [45]. The site for nucleophilic attack is on atom which has the highest value of f^{+}_{k}. In turn, the site for electrophilic attack is located on atom which has the highest value of f^{-}_{k} [17]. The values of the Fukui functions of all the nine imidazoline molecules are shown in Table 4. For molecules 1-7, only the nitrogen and carbon atoms in imidazole ring and hydrophilic group are listed. While for molecules 8-9, all non-hydrogen atoms are tabulated. As shown in Table 4, carbonatoms connected to nitrogen atom in hydrophilic group are the most reactive sites for nucleophilic attacks of all the molecules except for molecules 8 and 9. While, the most reactive sites for an electrophilic attack

are located on N5 in the imidazole ring except for molecules 7 and 9.

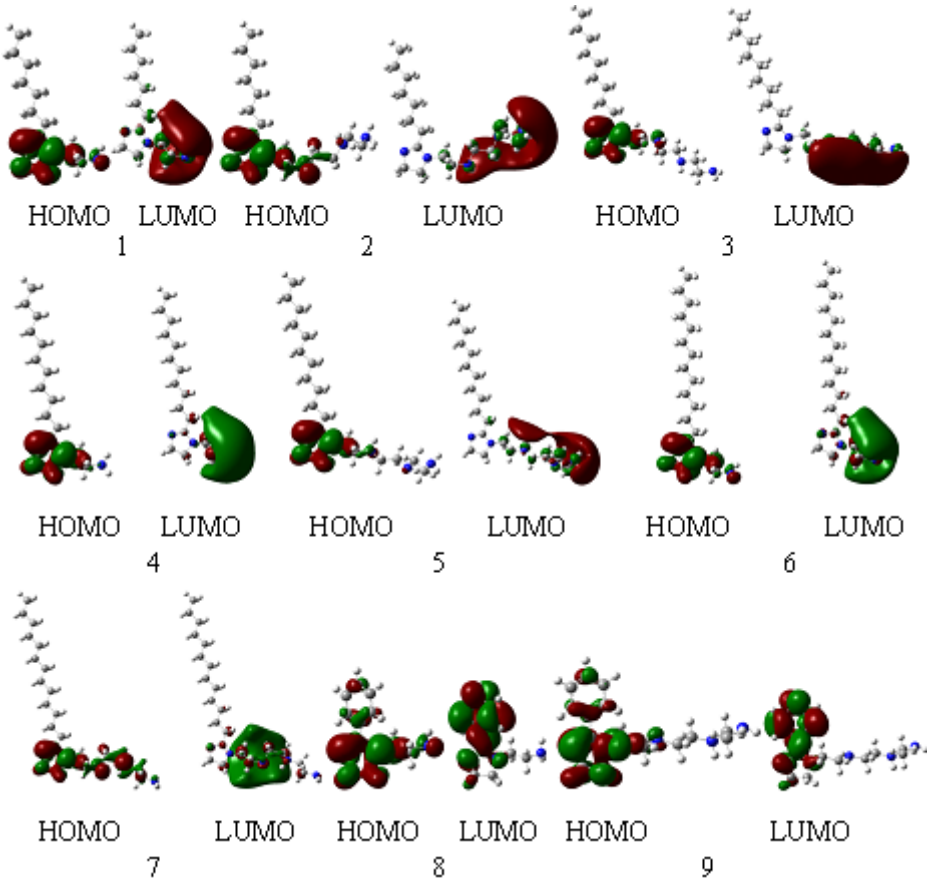

Figure1. The highest occupied molecular orbital (HOMO) and the lowest unoccupied molecular orbital (LUMO) of nine imidazoline molecules at the B3LYP/6-311+G (d,p) level of theory

Table 4. The condensed Fukui functions on the heavy atoms of imidazole ring and hydrophilic group of nine imidazoline molecules at the B3LYP/6-311+G (d,p) level of theory

1			2			3		
Atom	$f_i(\vec{r})^+$	$f_i(\vec{r})^-$	Atom	$f_i(\vec{r})^+$	$f_i(\vec{r})^-$	Atom	$f_i(\vec{r})^+$	$f_i(\vec{r})^-$
C1	0.005	0.004	C1	-0.001	0.009	C1	-0.004	0.008
C2	-0.030	0.019	C2	-0.045	0.008	C2	-0.063	0.015
N5	0.011	-0.252	N5	0.015	-0.140	N5	0.018	-0.196
N6	-0.043	-0.212	N6	-0.034	-0.117	N6	-0.024	-0.162
C7	-0.300	0.017	C7	-0.168	-0.007	C28	-0.005	0.024
C10	-0.106	-0.010	C10	-0.026	0.007	C38	-0.001	0.016
N13	-0.078	-0.101	N13	-0.017	-0.132	C41	-0.278	-0.003
C36	0.004	0.035	C36	0.001	0.017	N44	-0.031	-0.144
			C40	-0.016	0.005	C46	-0.133	0.016
			C43	-0.024	-0.002	C49	-0.043	0.006
			N46	0.001	-0.124	N52	-0.010	-0.030
			C48	-0.010	0.006	C54	-0.010	0.004
			C51	-0.295	-0.011	C57	-0.043	0.003
			N54	-0.040	-0.004	N60	-0.025	-0.025

Table 4(continued). The condensed Fukui functions on the heavy atoms of imidazole ring and hydrophilic group of nine imidazoline molecules at the B3LYP/6-311+G (d,p) level of theory

4			5			6		
Atom	$f_i(\vec{r})^+$	$f_i(\vec{r})^-$	Atom	$f_i(\vec{r})^+$	$f_i(\vec{r})^-$	Atom	$f_i(\vec{r})^+$	$f_i(\vec{r})^-$
C1	0.000	0.004	C1	0.002	-0.002	C1	0.004	0.004
C2	-0.028	0.019	C2	-0.001	0.012	C2	-0.022	0.019
N5	0.017	-0.251	N5	0.014	-0.197	N5	0.012	-0.252
N6	-0.028	-0.214	N6	-0.022	-0.162	N6	-0.039	-0.213
C7	-0.032	0.026	C7	-0.090	0.017	C7	-0.281	0.017
C10	-0.321	-0.006	C10	-0.033	-0.003	C10	-0.100	-0.010
N13	-0.080	-0.109	N13	-0.017	0.000	N13	-0.075	-0.100
C49	0.001	0.036	C48	0.001	0.028	C45	0.002	0.035
			C52	-0.006	-0.005			
			C55	-0.068	0.012			
			N58	-0.009	-0.155			
			C60	-0.060	0.012			
			C63	-0.122	0.003			
			N66	-0.045	-0.016			

Table 4(continued). The condensed Fukui functions on the heavy atoms of imidazole ring and hydrophilic group of nine imidazoline molecules at the B3LYP/6-311+G (d,p) level of theory

7			8			9		
Atom	$f_i(\vec{r})^+$	$f_i(\vec{r})^-$	Atom	$f_i(\vec{r})^+$	$f_i(\vec{r})^-$	Atom	$f_i(\vec{r})^+$	$f_i(\vec{r})^-$
C1	0.006	0.129	C1	-0.085	-0.008	C1	0.108	0.008
C2	-0.013	0.018	C2	-0.001	0.014	C2	0.092	-0.136
N5	0.014	-0.032	N5	-0.030	-0.229	N7	0.293	-0.009
N6	-0.035	-0.105	N6	-0.126	-0.220	C8	-0.210	-0.150
C7	-0.153	0.109	C7	-0.001	0.016	N9	0.259	0.011
C10	-0.056	-0.073	C10	0.001	-0.005	C10	0.086	-0.001
N13	-0.025	0.008	N13	-0.011	-0.073	C13	0.088	0.001
C45	0.003	-0.065	C15	0.017	0.040	N16	0.340	0.002
C58	-0.015	0.026	C19	-0.095	0.043	C18	0.089	0.010
C61	-0.143	-0.056	C20	-0.074	-0.013	C21	0.091	-0.128
N64	0.001	-0.028	C21	-0.058	-0.028	N24	0.340	0.000
C66	-0.030	-0.023	C22	-0.028	-0.015	C26	0.094	-0.003
C69	-0.026	0.018	C24	-0.034	-0.015	C29	0.103	-0.062
N72	0.001	-0.032	C26	-0.157	-0.057	N32	0.426	0.027
						C35	0.070	-0.007
						C36	0.114	-0.019
						C37	0.108	-0.008
						C38	0.076	-0.011
						C40	0.075	-0.037
						C42	0.148	0.023

Additionally, the active sites of imidazoline molecules were further studied by analysis of the contribution to HOMO and LUMO of atoms [41]. The most reactive site to donate electrons is the atom which has the highest value of the contribution to HOMO (χ^r_{HOMO}) and the most reactive site to accept electrons is the atom which has the highest value of the contribution to LUMO (χ^r_{LUMO}).The

values of the contribution to HOMO and LUMO of all the nine imidazoline molecules are presented in Table 5. For molecules 1-7, only nitrogen and carbon atoms in imidazole ring and hydrophilic group are listed, and for molecules 8 and 9, all non-hydrogen atoms are tabulated. As shown in Table 5, for χ^r_{HOMO}, the highest value is on N5 atom in the imidazole ring for the molecules 1-8, and on N7 atom in the imidazole ring for molecule 9. While for χ^r_{LUMO}, the highest value is located on the carbon atom connected to nitrogen atoms in hydrophilic group for molecules 1-7, and on carbon atoms in benzene ring for molecules 8 and 9. Therefore, for imidazoline molecules with alkyl chain, nitrogen atom connected to hydrophilic group in the imidazole ring is the active center and can donate electrons to metal in the adsorption process. At the same time, the carbon atoms in hydrophilic group can accept electrons from metal. However, for imidazoline molecules with benzene ring, the hydrophilic group is not the reactive region. These results are in accord with the results of the condensed Fukui function.

Table 5. The contribution to HOMO and LUMO on the heavy atoms of imidazole ring and hydrophilic group of nine imidazoline molecules at the B3LYP/6-311+G (d,p) level of theory

1			2			3		
Atom	χ^r_{HOMO}	χ^r_{LUMO}	Atom	χ^r_{HOMO}	χ^r_{LUMO}	Atom	χ^r_{HOMO}	χ^r_{LUMO}
C1	0.062	0.036	C1	0.102	0.077	C1	0.042	0.028
C2	0.011	0.002	C2	0.012	0.002	C2	0.008	0.011
N5	0.187	0.003	N5	0.212	0.003	N5	0.128	0.004
N6	0.092	0.000	N6	0.100	0.001	N6	0.064	0.000
C7	0.028	0.236	C7	0.030	0.133	C28	0.015	0.007
C10	0.038	0.127	C10	0.030	0.048	C38	0.027	0.071
N13	0.010	0.022	N13	0.053	0.013	C41	0.039	0.197
C36	0.017	0.000	C36	0.012	0.001	N44	0.008	0.006
			C40	0.005	0.019	C46	0.001	0.209
			C43	0.005	0.004	C49	0.003	0.316
			N46	0.002	0.005	N52	0.000	0.031
			C48	0.003	0.005	C54	0.001	0.013
			C51	0.002	0.056	C57	0.001	0.039
			N54	0.000	0.051	N60	0.000	0.011

Table 5(continued). The contribution to HOMO and LUMO on the heavy atoms of imidazole ring and hydrophilic group of nine imidazoline molecules at the B3LYP/6-311+G (d,p) level of theory

4			5			6		
Atom	χ^r_{HOMO}	χ^r_{LUMO}	Atom	χ^r_{HOMO}	χ^r_{LUMO}	Atom	χ^r_{HOMO}	χ^r_{LUMO}
C1	0.066	0.126	C1	0.075	0.039	C1	0.055	0.048
C2	0.011	0.008	C2	0.013	0.007	C2	0.012	0.002
N5	0.163	0.009	N5	0.199	0.002	N5	0.155	0.004
N6	0.081	0.001	N6	0.100	0.000	N6	0.075	0.000
C7	0.017	0.065	C7	0.036	0.198	C7	0.021	0.248
C10	0.014	0.077	C10	0.020	0.058	C10	0.032	0.140
N13	0.001	0.066	N13	0.005	0.016	N13	0.008	0.024
C49	0.034	0.007	C48	0.040	0.014	C45	0.024	0.000

	C52	0.006	0.031
	C55	0.007	0.007
	N58	0.002	0.010
	C60	0.000	0.004
	C63	0.000	0.078
	N66	0.000	0.031

Table 5(continued). The contribution to HOMO and LUMO on the heavy atoms of imidazole ring and hydrophilic group of nine imidazoline molecules at the B3LYP/6-311+G (d,p) level of theory

7			8			9		
Atom	χ^r_{HOMO}	χ^r_{LUMO}	Atom	χ^r_{HOMO}	χ^r_{LUMO}	Atom	χ^r_{HOMO}	χ^r_{LUMO}
C1	0.058	0.073	C1	0.048	0.108	C1	0.008	0.011
C2	0.012	0.006	C2	0.013	0.018	C2	0.013	0.019
N5	0.188	0.005	N5	0.222	0.006	N7	0.148	0.006
N6	0.086	0.001	N6	0.136	0.008	C8	0.042	0.072
C7	0.060	0.224	C7	0.068	0.019	N9	0.243	0.003
C10	0.095	0.113	C10	0.053	0.004	C10	0.024	0.104
N13	0.063	0.008	N13	0.016	0.001	C13	0.026	0.050
C45	0.014	0.000	C15	0.008	0.007	N16	0.009	0.001
C58	0.013	0.082	C19	0.016	0.104	C18	0.008	0.002
C61	0.024	0.080	C20	0.143	0.102	C21	0.007	0.000
N64	0.088	0.002	C21	0.046	0.503	N24	0.000	0.000
C66	0.003	0.006	C22	0.098	0.011	C26	0.000	0.001
C69	0.013	0.000	C24	0.037	0.062	C29	0.000	0.000
N72	0.003	0.001	C26	0.023	0.043	N32	0.000	0.000
						C35	0.008	0.085
						C36	0.152	0.128
						C37	0.082	0.418
						C38	0.081	0.008
						C40	0.044	0.057
						C42	0.023	0.029

3.4 Molecular dynamics simulation

The molecular dynamics simulation was performed to study the adsorption behavior of the imidazoline molecules on the Fe surface. The geometry of the studied system was being optimized until the total energy was minimized and then molecular dynamics simulation process was carried out. The studied system reached equilibrium when both of temperature and energy of the system were balance. The values of the interaction energies and the binding energies of all the nine imidazoline molecules on Fe surface were calculated after the systems reached equilibrium. The equilibrium configurations of the nine imidazoline molecules adsorbed on Fe(110) surface are presented in Figure 2. And the calculated binding energies are shown in Table 6.

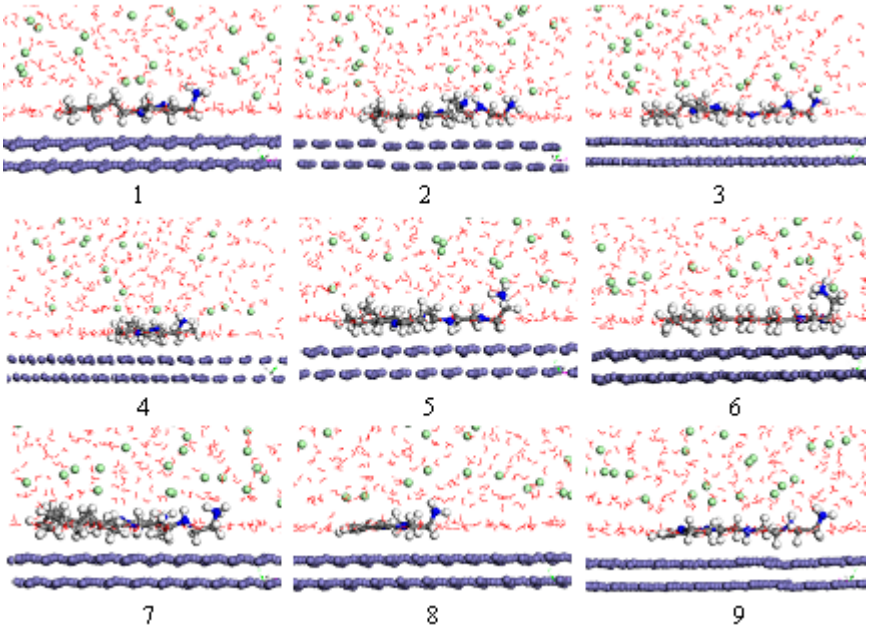

Figure 2. Equilibrium configuration of nine imidazoline molecules adsorbed on Fe(110) surface

As shown in Figure.2, almost all the imidazoline molecules were adsorbed on the Fe(110) surface in parallel manner, which indicates that not only imidazoline ring and hydrophilic group but also the hydrocarbon straight-chain can be absorbed on the Fe surface. However, the protonated amino group, $-NH_3^+$, was not likely adsorbed on iron surface, which was possible due to electron deficient nature of the protonated N atom. Calculation of single point energy of E_{total}, $E_{surface}$ and $E_{inhibitor}$ was carried out by using the Forcite module, and $E_{interaction}$ and $E_{binding}$ can be obtained according to the following equations [17-18]:

$$E_{interaction} = E_{total} - (E_{surface} + E_{inhibitor}) \quad (1)$$

$$E_{binding} = - E_{interaction} \quad (2)$$

where E_{total} is the total energy of iron crystal together with the adsorbed imidazoline molecule, $E_{surface}$ and $E_{inhibitor}$ are the energy of the iron crystal and imidazoline molecule, respectively. The calculated binding energies and experimental inhibition efficiencies are listed in Table 6.

Table 6. Binding energies and inhibition efficiencies of nine imidazoline molecules

Inhibitor	Binding energy (Kcal/mol)	Inhibition efficiency (%)	Inhibitor	Binding energy (Kcal/mol)	Inhibition efficiency (%)
1	125.32	26.34	6	178.43	60.64
2	175.50	87.71	7	225.04	57.67
3	189.92	91.59	8	106.60	20.62
4	161.99	77.86	9	160.28	59.01
5	207.26	95.39			

According to studies about the interactions between corrosion inhibitor and metal surface [17-18], the bigger value of $E_{binding}$ is, the easier of the corrosion inhibitor can be adsorbed on the surface, and the higher inhibition efficiency of the molecule will has. The relationship between the binding

energies and inhibitor efficiencies of nine imidazoline molecules are presented in Figure 3. As shown in Figure 3, the order of $E_{binding}$ of imidaoline molecules accords well with the trend of inhibition efficiencies. It can be concluded that the binding energy is a good indicator of the inhibition efficiency.

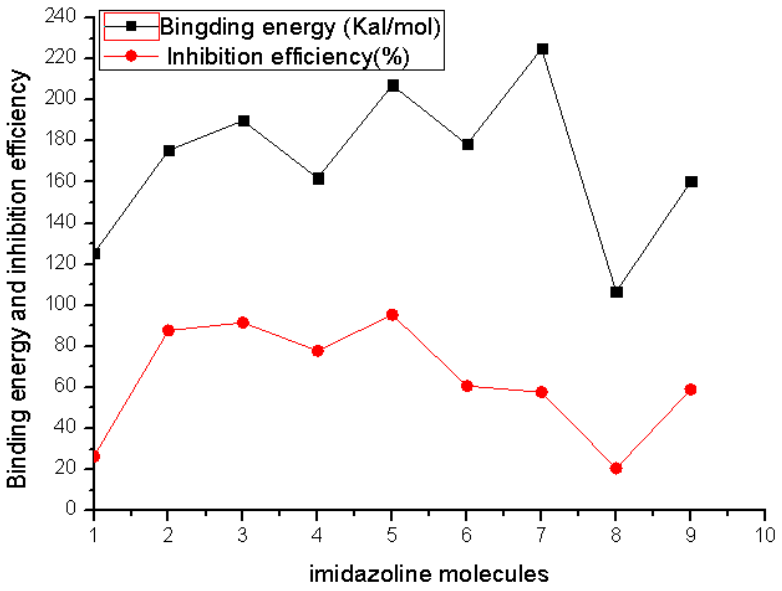

Figure 3. The relationship between binding energies and inhibition efficiencies of nine imidazoline molecules

3.5 Quantitative structure and activity relationship (QSAR)

In the present study, the support vector machine (SVM) approach has been used to build quantitative structure and activity relationship (QSAR) between the inhibition efficiencies of the imidazoline inhibitors and the structural characters. All the quantum chemical parameters calculated by DFT method, binding energies calculated by molecular dynamics method and inhibitor efficiencies tested by weight-loss method of the nine imidazoline molecules have been as inputs to build a QSAR model (shown in Table 3). The eventual result was a mathematical complex expression which was not an explicit equation or function. The accuracy of the model was indicated by the correlation coefficient R^2. High R^2 value indicates the great success and predictive power of the model [35]. In the present study, SVM gives the correlation coefficient 0.976 for the model built, which shows good performance. And the parameters of SVM for regression, c and γ, were fixed to 4 and 0.1, respectively. Figure 4 shows a comparison between the predicted values and the original data of inhibition efficiencies. The results predicted from model are very close to the results obtained from experiment. The deviation of the predicted values from original value was described in Figure 5. The values of the deviation were less than 0.4%. As shown in Figure 6, the relative errors between the predicted values and the original values were less than 2%. These results indicated that a good model have been built by SVM approach.

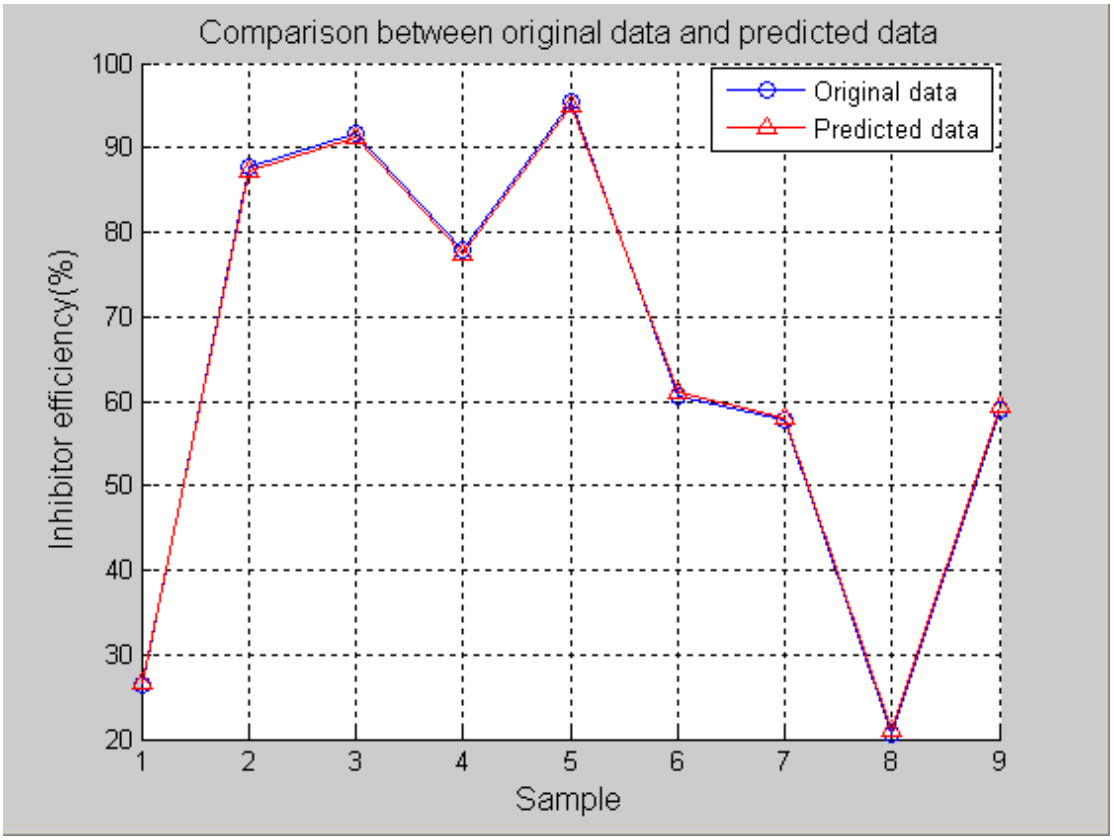

Figure 4. Comparison between the original and predicted data of nine imidazoline molecules

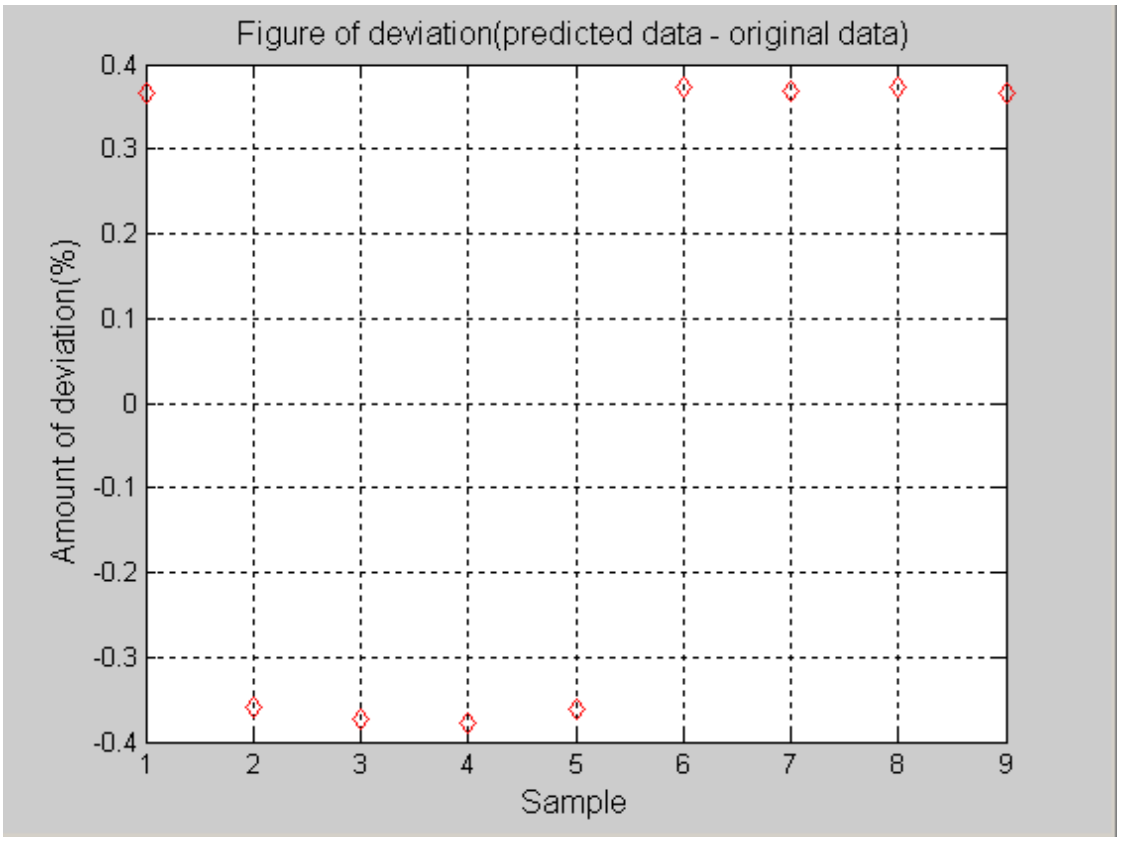

Figure 5. Deviation between the predicted and original data of nine imidazoline molecules

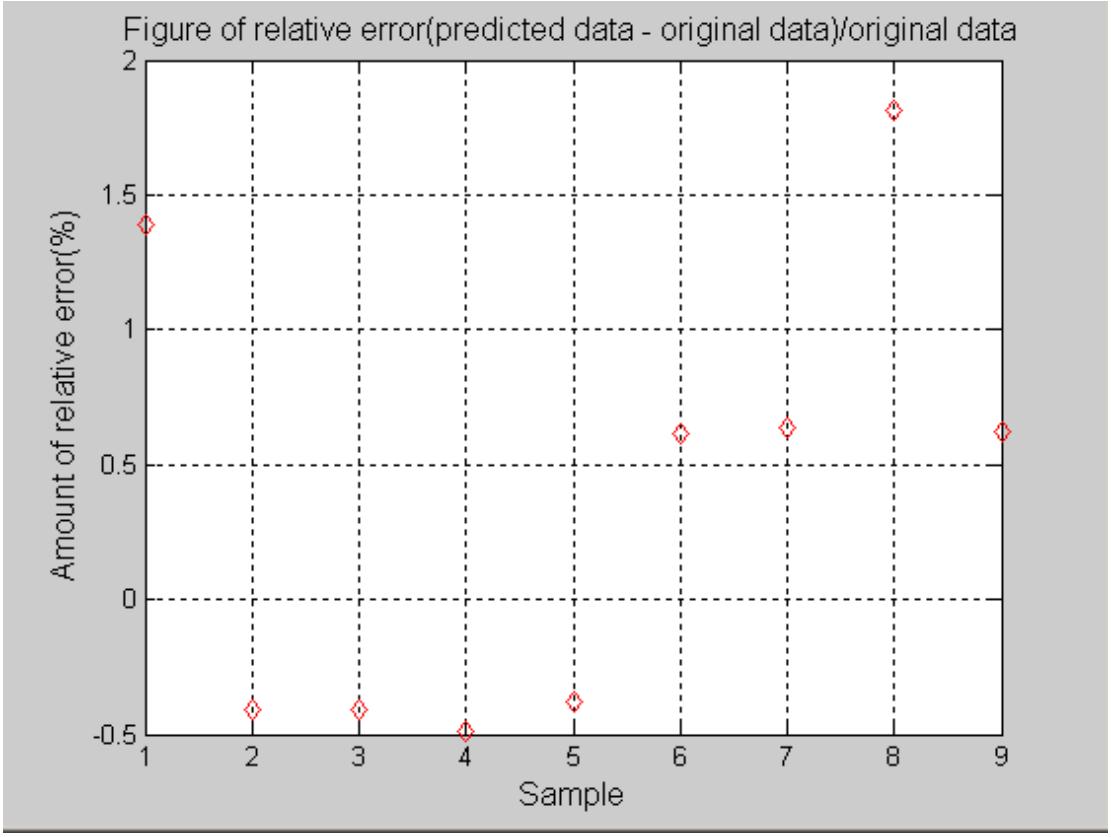

Figure 6. Relative error between the predicted and original data of nine imidazoline molecules

3.6 Molecular design and prediction

Table 7. Structures of eight theoretically designed imdazoline molecules

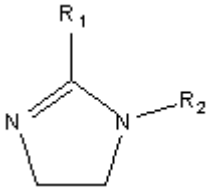

Inhibitor	R_1	R_2
1	—$(CH_2)_8$-CH=CH	—$CH_2CH_2NH_2$
2	—$(CH_2)_8$-CH=CH	—$(CH_2CH_2NH)_2CH_2CH_2NH_2$
3	—CH=CH-$(CH_2)_8$-CH_3	—$CH_2CH_2NH_2$
4	—CH=CH-$(CH_2)_8$-CH_3	—$(CH_2CH_2NH)_2CH_2CH_2NH_2$
5	—CH=CH-$(CH_2)_9$-CH_3	—$CH_2CH_2NH_2$
6	—CH=CH-$(CH_2)_9$-CH_3	—$(CH_2CH_2NH)_2CH_2CH_2NH_2$
7	—$(CH_2)_7$CH=CH-$(CH_2)_3$-CH_3	—$CH_2CH_2NH_2$
8	—$(CH_2)_7$CH=CH-$(CH_2)_3$-CH_3	—$(CH_2CH_2NH)_2CH_2CH_2NH_2$

Eight new imidazoline molecules were theoretically designed and their structures were presented in Table 7. As shown in Table 7, the hydrophilic groups of the eight new designed molecules

were the same as those of experimental imidazoline molecules. While for the hydrophobic groups, four different hydrophobic alkenyl chains, which can be commercially got easily, were taken into consideration.

The structures of all the new molecules were optimized at the B3LYP/6-311+G (d,p) level of theory, and their corresponding quantum chemical parameters/descriptors were listed in Table 9. At the same time, the adsorption behaviors of these new molecules on the Fe(110) surface were studied by molecular dynamics simulation, and the binding energies were also presented in Table 8. The calculated quantum chemical parameters as well as the binding energies were taken as inputs into the established QSAR model, which provided the predicted inhibition efficiencies as outputs (shown in Table 8). As we know, these data were just suitable for the test condition in 15 wt. % HCl and 3 wt. % HF solution with corrosion inhibitor concentration of 400 ppm at 60°C for 4 h. As shown in Table 8, the predicted inhibition efficiencies of all the new imidazoline molecules were from 34.950% to 81.382%. Molecule 1 was predicted the lowest inhibition efficiency, 34.950% and molecule 2 was predicted the highest inhibition efficiency, 81.382%. Moreover, it is found that the predicted inhibition efficiencies of new imidazoline molecules with hydrophilic group of $-(CH_2CH_2NH)_2CH_2CH_2NH_2$ are higher than those of $-CH_2CH_2NH_2$, which was in accordance with the trend of the experimental molecules discussed above. Inhibition mechanism and molecular design are very complicated. We hope that the obtained results can provide some useful clues to the study of the corrosion inhibitor in the future.

Table 8. Quantum chemical parameters of eight theoretically designed imidazoline molecules at the B3LYP/6-311+G(d,p) level of theory and predicted inhibition efficiencies

Inhibitor	E_{homo}/eV	E_{lumo}/eV	μ/Debye	α	Q_{total}/C	Q_{ring}/C	Z_{total}/C	Z_{ring}/C
1	-5.859	-0.200	3.581	208.620	-6.335	-0.998	-4.676	-0.440
2	-5.831	-0.144	4.426	278.350	-8.411	-0.999	-6.055	-0.426
3	-5.728	-0.866	2.516	227.110	-6.651	-1.026	-4.956	-0.800
4	-5.744	-0.868	3.595	297.490	-8.707	-1.021	-6.507	-0.592
5	-5.729	-0.867	2.564	239.670	-7.026	-1.026	-5.266	-0.806
6	-5.743	-0.869	3.515	310.160	-9.082	-1.022	-6.823	-0.584
7	-5.852	-0.194	3.206	248.800	-7.496	-0.998	-6.225	0.223
8	-5.863	-0.232	4.261	319.410	-9.552	-0.996	-7.162	-0.200

Table 8 (continued). Quantum chemical parameters of eight theoretically designed imidazoline molecules at the B3LYP/6-311+G(d,p) level of theory and predicted inhibition efficiencies

Z_{ring}/C	V/cm^3mol^{-1}	AIP/eV	VIP/eV	EA_{vert}/eV	ΔN_{vert}	ΔN	E_{ad} kcal/mol^{-1}	Predicted IE/ %
-0.440	159.571	7.222	7.568	-0.718	0.431	0.674	-160.682	34.950
-0.426	211.713	7.073	7.382	-0.637	0.452	0.702	-149.231	81.382
-0.800	169.197	7.008	7.502	-0.547	0.438	0.762	-164.509	50.273
-0.592	221.339	6.922	7.254	-0.400	0.467	0.757	-216.048	59.060
-0.806	178.823	7.007	7.500	-0.552	0.438	0.761	-162.187	52.879
-0.584	230.965	6.920	7.252	-0.518	0.468	0.758	-218.227	59.818
0.223	188.450	7.127	7.735	-0.682	0.413	0.703	-170.617	43.794
-0.200	240.591	7.046	7.620	-0.564	0.424	0.702	-229.543	74.262

4. CONCLUSIONS

In the present study, the inhibition performance of nine imidazoline molecules was studied by weight-loss method, quantum chemical calculation, molecular dynamics simulation and the quantitative structure−activity relationship (QSAR) analysis. What's more, eight new imidazoline molecules were theoretically designed and their inhibition efficiencies were predicted. The main conclusions are as following:

(1) For the imidazoline molecules with hydrocarbon straight-chain, the inhibition efficiencies were not always increase with the increasing of the lengths of straight-chain. In addition, for the imidazoline molecules with the same hydrophobic groups, the inhibition efficiencies with $-(CH_2CH_2NH)_2CH_2CH_2NH_2$ are higher than those with $-CH_2CH_2NH_2$.

(2) Though all the quantum chemical parameters of these imidazoline molecules discussed in the present paper are related to the chemical reactivity, the order of each parameter does not correlate well with the trend of the inhibition efficiency.

(3) Local reactivity results according to the distribution of HOMO and LUMO, the condensed Fukui function and contribution to HOMO and LUMO of atoms indicate that the nitrogen atoms in the imidazole ring and carbon atoms in hydrophilic group were the possible active sites to be adsorbed on iron surface.

(4) The acid solution was taken into consideration in molecular dynamics simulation and the results indicate that all the imidazoline molecules can be adsorbed on Fe surface due to that the values of the binding energies were all positive. And the order of binding energies agrees well with that of inhibitor efficiencies. What's more, almost all the nine imidazoline molecules were adsorbed on the Fe(110) surface in parallel manner in acidic solution.

(5) The quantitative structure and activity relationship (QSAR) model built by the support vector machine (SVM) approach, in which all the calculated quantum chemical parameters and the binding energies were taken as the descriptors, shows the good performance since the correlation coefficient R^2 was reasonably high. Eight new imidazoline molecules were theoretically designed and their inhibition efficiencies were predicted by this QSAR model.

ACKNOWLEDGMENTS

We are indebted to the projects funded key construction branch of China National Petroleum Corporation, scientific research and technological development(2011GJTC-09-01) and Scientific research and technological development project of the China National Petroleum Corporation(2011E-2505), special projects funded national science and technology(2011ZX-05059-004), Chinese National Natural Science Foundation (20903010, 21243008, 50904061 and 61201352), Beijing Municipal Natural Science Foundation (2132035), Opening Project of State Key Laboratory of Explosion Science of Technology (Beijing Institute of Technology) (2DkT10-01a and ZDKT12-03) for support of this research.

References

1. E.-S. M. Sherif, R. M. Erasmus, J. D. Comins, *Electrochim. Acta* 55 (2010) 3657
2. I. B. Obot, N. O. Obi-Egbedi, *Corros. Sci.* 52 (2010) 198

3. A. Kokalj, S. Peljhan, M. Finsgar, I. Milosev, *J. Am. Chem. Soc.* 132 (2010) 16657
4. E. E. Ebenso, M. M. Kabanda, T. Arslan, M. Saracoglu, F. Kandemirli, d L. C. Murulana, *Int. J. Electrochem. Sci.* 7 (2012) 5643
5. L. D. Paolinelli, T. Perez, S. N. Simison, *Mater. Chem. Phys.*126 (2011) 938
6. L. M. Rivera-Grau, M. Casales, I. Regla, *Int. J. Electrochem. Sci.* 7 (2012) 12391
7. J. Cruz, L.M. R. Aguilera, R. Salcedo, M. Castro, *Intern. J. Quantum Chem.* 85 (2001) 546
8. J. Zhang, X.L. Gong, H.H. Yu, M. Du, *Corros. Sci.* 53 (2011) 3324
9. P. C. Okafor, C. B. Liu, Y. J. Zhu, Y. G. Zheng, *Ind. Eng. Chem. Res.* 50 (2011) 7273
10. D. M. Ortega-Toledo, J. G. Gonzalez-Rodriguez, M. Casales, A. Cacere, L. Martinez, *Int. J. Electrochem. Sci.*, 6 (2011) 778
11. B. Wang, M. Du, J. Zhang, C. J. Gao, *Corros. Sci.* 53 (2011) 353
12. L. M. Rivera-Grau, M. Casales, I. Regla, *Int. J. Electrochem. Sci.* 8 (2013) 2491
13. L. M. Quej-Ake, R. Cabrera-Sierra, E. M. Arce-Estrada, *Int. J. Electrochem. Sci.* 8 (2013) 924
14. M. Mousavi, M. Mohammadalizadeh, A. Khosravan, *Corros. Sci.* 53 (2011) 3086
15. J. Cruz, L. M. R. Martinez-Aguilera, R. Salcedo, M. Castro, *Int J Quantum Chem.* 85 (2001) 546
16. J. Zhang, J. Liu, W. Yu, Y. Yan, L. You, L. Liu, *Corros. Sci.* 52 (2010) 2059
17. K.F. Khaled, *Electrochim. Acta* 55 (2010) 6523
18. S. Xia, M. Qiu, L. Yu, F. Liu, H. Zhao, *Corros. Sci.* 50 (2008) 2021
19. S. Hu, J. Hu, X. Shi, J. Zhang, W. Guo, *Acta Phys. -Chim. Sin.*25 (2009) 2524
20. Y. Tang, L. Yao, C. Kong, W. Yang, Y. Chen, *Corros. Sci.* 53 (2011) 2046
21. K.F.Khaled, N. A. Al-Mobarak, *Int. J. Electrochem. Sci*. 7 (2012) 1045
22. N.O. Obi-Egbedi, I.B. Obot, M.I. El-Khaiary, S.A. Umoren, E.E. Ebenso, *Int. J. Electrochem. Sci.* 6 (2011) 5649
23. M.J. Frisch, G.W. Trucks, H.B. Schlegel, G.E. Scuseria,M.A. Robb, J.R. Cheeseman, G. Scalmani, V. Barone, B. Mennucci, G.A. Petersson, H. Nakatsuji, M. Caricato, X. Li, H.P. Hratchian, A.F. Izmaylov, J. Bloino, G. Zheng, J.L. Sonnenberg, M. Hada, M. Ehara, K. Toyota, R. Fukuda, J. Hasegawa, M. Ishida, T. Nakajima, Y.Honda, O. Kitao, H. Nakai, T. Vreven, J. A. Montgomery, Jr., J.E. Peralta, F.Ogliaro, M. Bearpark, J.J. Heyd, E. Brothers, K.N. Kudin, V.N. Staroverov, R.Kobayashi, J. Normand, K. Raghavachari, A. Rendell, J.C. Burant, S.S. Iyengar, J. Tomasi, M. Cossi, N. Rega, J.M. Millam, M. Klene, J.E. Knox, J.B. Cross, V. Bakken, C. Adamo, J. Jaramillo, R. Gomperts, R.E. Stratmann, O. Yazyev, A.J. Austin, R. Cammi, C. Pomelli, J.W. Ochterski, R.L. Martin, K. Morokuma, V.G. Zakrzewski, G.A. Voth, P. Salvador, J.J. Dannenberg, S. Dapprich, A.D. Daniels, Ö. Farkas, J.B. Foresman, J.V. Ortiz, J. Cioslowski, D.J. Fox, Gaussian 09, Revision A.1, Gaussian, Inc., Wallingford CT, 2009
24. P. Senet, *Chem. Phys. Lett.* 275 (1997) 527
25. N. O. Eddy, B. I. Ita, *J. Mol. Model*. 17 (2011) 359
26. W. Xu, A. Gao, *J. Chem. Phys.* 123 (2005) 84320
27. R. G. Pearson, *Inorg. Chem.* 27 (1988) 734
28. A.Y. Musa, A.A.H. Kadhum, A. B. Mohamed, M. S. Takriff, *Mater. Chem. Phys.* 129 (2011) 660
29. A. Reed, L. Curtiss, F. Weinhold, *Chem. Rev.* 88 (1988) 899
30. R. G. Parr, W. T. Yang, *J. Am. Chem. Soc.* 106 (1984) 4049
31. S. Zhang, W. Lei, M. Xia, F. Wang, *THEOCHEM* 732 (2005) 173
32. A. Musa, R. Jalgham, A. Mohamad, *Corros. Sci.* 56 (2012) 176
33. S. Hu, A. Guo, Y. Geng, X. Jia, S. Sun, J. Zhang, *Mater. Chem. Phys.* 134 (2012) 54
34. K. F. Khaled, *Electrochim. Acta* 53 (2008) 3484
35. L. Tang, Y. Zhou, J. Jiang, H. Zou, H. Wu, G. Shen, *J. Chem. Inf. Model* 47 (2007) 1438
36. H. Golmohammadi, Z. Dashtbozorgi, W. Acree, *Eur. J. Pharm. Sci.* 47 (2012) 421
37. E. Byvatov, U. Fechner, J. Sadowski, G. Schneider, *J. Chem. Inf. Comput. Sci.* 43 (2003) 1882
38. G. Gece, S. Bilgic, *Corros. Sci.* 51 (2009) 1876
39. I.Ahamad, R. Prasad, M.A. Quraishi, *Corros. Sci.* 52 (2010) 1472

40. E. Sayed, H. E. Ashry, A. E. Nemr, S. Ragab, *J. Mol. Model.* 18 (2012) 1173
41. M. M Kabanda, L. C. Murulana, M.Ozcan, F. Karadag, I. Dehri , I.B. Obot , E.E. Ebenso, *Int. J. Electrochem. Sci.* 7 (2012) 5035
42. W.Li, Q.He, C Pei, B.Hou, *Electrochim. Acta* 52 (2007) 6386
43. L.M. Rodriguez,W. Villamisr, L. Martinez, Daniel Glossman-Matnik, *Corros. Sci.* 48 (2006) 4053
44. A. Musa, A. Kadhum, A. Mohamad, A. Rahoma, H. Mesmari, *J.Mol. Struct.* 969 (2010) 233
45. W. Yang,W.J. Mortier, *J. Am. Chem. Soc.* 108 (1986) 5708

© 2013 by ESG (www.electrochemsci.org)